RETRIEVING COSMOLOGICAL SIGNAL USING COSMIC FLOWS

V. Bouillot[1] and J.-M. Alimi[1]

Abstract. To understand the origin of the anomalously high bulk flow at large scales, we use very large simulations in various cosmological models. To disentangle between cosmological and environmental effects, we select samples with bulk flow profiles similar to the observational data Watkins et al. (2009) which exhibit a maximum in the bulk flow at 53 h^{-1} Mpc. The estimation of the cosmological parameters Ω_M and σ_8, done on those samples, is correct from the *rms* mass fluctuation whereas this estimation gives completely false values when done on bulk flow measurements, hence showing a dependance of velocity fields on larger scales. By drawing a clear link between velocity fields at 53 h^{-1} Mpc and asymmetric patterns of the density field at 85 h^{-1} Mpc, we show that the bulk flow can depend largely on the environment. The retrieving of the cosmological signal is achieved by studying the convergence of the bulk flow towards the linear prediction at very large scale ($\sim$ 150 h^{-1} Mpc).

Keywords: cosmology

1 Introduction

Velocity fields are unique probes for cosmology. Since it traces the growth of structures, velocity fields enable us to constraint dark energy models. Moreover, bulk flow (i.e. the dipole of the peculiar velocity fields) is a sensitive probe of matter fluctuation on large scales. Recent measurements (Watkins et al. 2009), based on the compositing of several peculiar velocity surveys, have exhibited a large deviation from the concordance ΛCDM model prediction. As a matter of fact, a convergence of the bulk flow toward the linear prediction of the ΛCDM model is far from being observed at 50 h^{-1} Mpc. This was claimed to be a challenge to ΛCDM.

A usual method to study the convergence of the velocity of the Local Group toward the CMB dipole is also to reconstruct peculiar velocities from redshift surveys using linear theory. A recent example is the reconstruction of the velocity fields of the 2MASS Redshift Survey (Erdoğdu et al. 2006). However, linear theory is not valid when dealing with large density fluctuations as the Virgo cluster or the Shapley cluster and may lead to anomalously high velocity fields. To obtain a better reconstruction of the velocity fields, a possible solution is to use Lagrangian methods, e.g. Monge-Ampère-Kantorovich method, which enable to better take into account the nonlinear regime. This issue has been widely developed by Lavaux et al. (2010). Those types of reconstruction are in agreement with Watkins et al. (2009), especially on the existence of a maximum in the bulk flow.

In this proceeding, we highlight the dependance of the bulk flow on the environment. This dependance must be carefully studied to understand the role of cosmology in the observed deviations from predicted velocity fields. To separate cosmological and environmental effects, we use very large simulations done according to various cosmological scenarii. In those simulations, we select samples with bulk flow profiles similar to the measurements of Watkins et al. (2009) (see Fig. 1). We first describe the numerical simulations used in this study as well as the method used to compute observables. In a second part, we introduce the notion of density field asymmetry in spheres. This enables us to describe the environmental dependance of the bulk flow at intermediate scales. Finally, we conclude in section 4 with a brief discussion and summary.

[1] Laboratoire Univers et Théories (LUTh), UMR 8102 CNRS, Observatoire de Paris, Université Paris Diderot, 5 place Jules Janssen, 92190 Meudon, France

Parameters	ΛCDM	RPCDM	SUCDM
Ω_m	0.26	0.23	0.25
α	0	0.5	1
σ_8^{lin}	0.80	0.66	0.73
w_0	-1	-0.87	-0.94
w_1	0	0.08	0.19

Table 1. Cosmological parameters selected for the realistic models. These are flat models ($\Omega_{Q(\Lambda)} = 1 - \Omega_m$), with a spectral index $n_s = 0.963$, $A_S = 2.1 \times 10^{-9}$, $h = 0.72$, $\Omega_b h^2 = 0.02273$, and $\tau = 0.087$.

2 Numerical set-up

2.1 The Dark Energy Universe Simulation Series

The Dark Energy Universe Simulation Series (Alimi et al. 2010; Rasera et al. 2010) is a series of N-body simulations realized in three different realistic cosmological scenarii namely ΛCDM model, Ratra-Peebles and Supergravity quintessence models. The cosmological parameters used in those simulations are fixed in order to have realistic cosmological models (i.e. in agreement with SNe, CMB and BAO). Their values, fitted on the CMB and supernovae data with a likelihood analysis, are given in Table 1. The simulations followed 1024^3 dark matter particles from z = 92 to the present day within a cubic region of $648h^{-1}$ Mpc on a side. About 0.5 million dark matter haloes that contain more than 100 particles are detected at z = 0 according to a friends-of-friends (FOF) algorithm with a linking lenght $b = 0.2$ (Davis et al. 1985). In this proceeding, we present the analysis on ΛCDM only. The inclusion of other cosmologies will be done in a forthcoming paper (Alimi et al. in prep).

2.2 Computing numerical bulk flow

The peculiar velocity of galaxies $\mathbf{u}$ can be seen as the departure from an idealized isotropic expansion and thus can be expressed as a sum of two terms: $\mathbf{u}(\mathbf{r}) = \mathbf{u}(0) + \mathbf{v}(\mathbf{r}) - H_0\mathbf{r}$, with $\mathbf{v}(\mathbf{r})$ representing the global motion of galaxies and $H_0\mathbf{r}$ the mean Hubble expansion. The bulk (i.e. volume average) flow is defined as the mean of $\mathbf{v}(\mathbf{r})$ in a sphere of growing radius.

Having the tridimensional velocity fields of N_h objects in a sphere of radius R centered on the Local Group, observers can express the bulk flow as:

$$v_{bulk}(R) = \left\| \frac{1}{N_{h,r<R}} \sum_i^{N_h, r<R} \vec{v}_i \right\| \tag{2.1}$$

This quantity can be computed exactly in numerical simulations. We choose to throw randomly 20,000 centers in the computational volume and compute bulk flows in increasing radii for each of these centers.

A statistical definition of the bulk flow, formally equivalent to the root mean square mass fluctuation σ_R, can be given:

$$v_{bulk} = \sqrt{<\bar{v}^2>} = \sqrt{\frac{1}{2\pi^2} \int_0^\infty dk \ k^2 P_v(k) \hat{W}(kR)^2} \tag{2.2}$$

This definition is of utmost importance since it links the velocity power spectrum to the bulk flow, doing a statistical mean on all possible environments. Therefore, a departure from this prediction is deeply linked with environmental effects.

From our 20.000 objects (i.e. centers), we extract two subsets:

1. Centers with a bulk flow close to the linear prediction (at 95% confidence level);

2. Centers with a bulk flow close to the observational data based on the measurements of Watkins et al. (2009) (at 95% confidence level). This sample is called *realistic* since its mean bulk flow profile is in agreement with the observations with specially a minimum at 16 h^{-1} Mpc and a bump at 53 h^{-1} Mpc (Fig. 1 right).
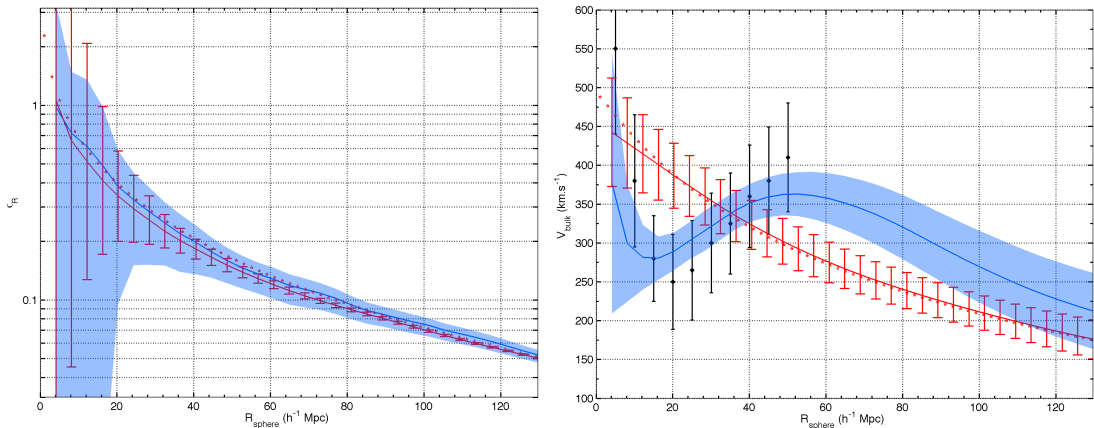
Fig. 1. Left: σ_R vs the radius of spheres. **Right**: Bulk flow vs radius of spheres. The linear prediction is shown with red stars, the linear subset is in red and the realistic sample in blue. Error bars correspond to the scattering of the bulk flows.

Computing mean and standard variances of the bulk flow and the *rms* mass fluctuation for both classes, we obtain Figure 1. On this figure, we see clearly the agreement between the mean behavior of the realistic (blue) and the observational (red) data for the σ_R and the strong disagreement between the realistic data and the linear prediction for the bulk flow.

Such a discrepancy finds its origin in the definition of the matter and velocity fields. In fact, the *rms* mass fluctuation is undistinguishable from one subset to the other one since it only keeps track of local overdensities. Since the density contrast is not very sensitive to large scales, it converges quickly towards the linear prediction and both subsets have the same behavior. On the contrary, the bulk flow, computed from vectorial quantities, has kept the imprint of the directional information: it gives an hint on the amplitude of the density field. Therefore, we have to quantify the position of overdensities in a given direction with respect to the opposite direction i.e. the asymmetry of the matter field in a sphere.

3 Environmental effects

The asymmetry in a sphere of (equivalently in a shell at) radius R_0 is defined by a vector which norm (named the asymmetry index) can be defined mathematically as followed:

$$A_{R_0} = \max_{\phi_0 \in [0,2\pi], \theta_0 \in [0,2\pi]} \left\{ \frac{1}{\rho_{mean}} \iint_{S^2/2} \rho_{<R_0}(\theta + \theta_0, \phi + \phi_0) - \rho_{<R_0}(\pi - (\theta + \theta_0), \pi + (\phi + \phi_0)) d\Omega \right\}, \quad (3.1)$$

ρ_A being the density in a shell at radius A, $\rho_{<R_0}$ the density from 0 to radius R_0 and (θ, ϕ) the direction of the density field.

Physically, the asymmetry index characterizes the deviation from a symmetric sphere. A symmetric environment will be characterized by an asymmetry index equal to zero whereas an highly asymmetric environment exhibits an asymmetry index close to one. The direction of the asymmetry corresponds to find the direction of the densest hemisphere, which is a function of ϕ_0 and θ_0 [*].

The numerical computation of the mean asymmetry index (Figure 2) exhibits three zones. From 12 to 40 h^{-1} Mpc, the observational set and the linear sample show the same tendency i.e. a linear behavior. From 40 to 76 h^{-1} Mpc, the observational subset is more symmetric than the linear sample. Finally, from 76 to 128 h^{-1} Mpc, the observational subset is more asymmetric than the linear sample. Since matter sources velocity fields, the latter should therefore be linked with the bump of the bulk flow. In fact, an alignment of the bulk flow and the asymmetry should be observed at large scales. This link is particularly enhanced between the scale of the

---

[*]This issue as well as the equivalence between the characterization of the environment by the center of mass or the asymmetry index will be discussed in a forthcoming paper (Bouillot et al. in prep). Intuitively, the more symmetric a sphere is, the nearer the center of mass to the geometric center is.
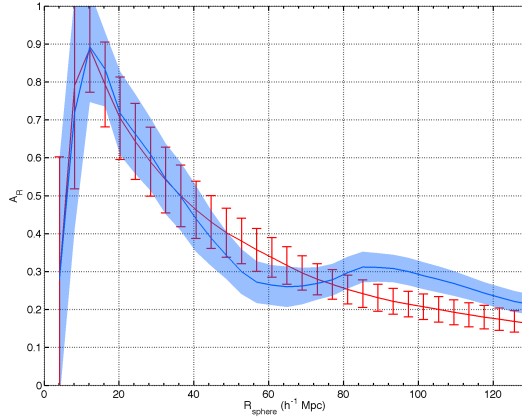
Fig. 2. Asymmetry index vs radius of the sphere for realistic subsets.
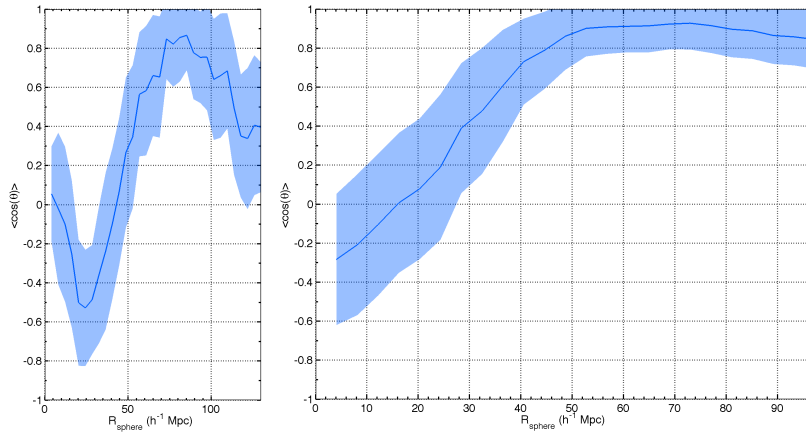

Fig. 3. Asymmetry index vs radius of the sphere for linear (red) and realistic (blue) subsets.

maximum of the bulk flow and the scale of the maximum of the asymmetry index.

To exhibit this alignment scale of the asymmetry vector and the bulk flow at 53 h^{-1} Mpc, we compute the normalized scalar product of the bulk flow at 53 h^{-1} Mpc and the asymmetry in a shell (instead of a sphere). This will show the sourcing scale of the bulk flow. Left panel of Figure 3 gives the value of this particular scale: 85 h^{-1} Mpc [†].

Once the bulk flow is aligned at high scales, the direction of the bulk flow remains roughly the same. As a matter of fact, the direction of the bulk flow should remain aligned with the direction of the asymmetry at higher scales. Performing a shift δR of the asymmetry index, the alignment of the bulk flow along the direction of the asymmetry at higher scale can be visualized. This is shown on the right panel of Figure 3 with the computation of the scalar product of the bulk flow at radius R and the asymmetry in a sphere at radius R+δR with $\delta R = 32 \pm 4.1$ h^{-1} Mpc.

4   Conclusion

By building samples with bulk flow profiles in agreement with the observations, we show that the anomalously high bulk flow detected in observational datasets is mainly due to environmental effects. Those effects are shown by quantifying the asymmetric tridimensional distribution of matter. In particular, a bump of the bulk

---

[†]The fact that this scale corresponds exactly to the scale of the maximum of the asymmetry index is pure luck and do not have any physical meaning.

flow at 53 h^{-1} Mpc is explained by an asymmetric distribution of matter at 85 h^{-1} Mpc. The major result is that, by studying the distribution of matter, one can infer the position of the maximum of the bulk flow, hence constraining cosmological models. In other words, the study of the matter field of redshifts surveys can give us the scale of the position of the maximum of the bulk flow without ultra-deep velocity surveys. Far from this scale, a convergence towards the linear prediction is observed and therefore, only the cosmological signal remains (Alimi et al. in prep).

References

Alimi, J.-M., Bouillot, V., Füzfa, A., & Rasera, Y. 2012, MNRAS (in prep)

Alimi, J.-M., Füzfa, A., Boucher, V., et al. 2010, MNRAS, 401, 775

Bouillot, V., Alimi, J.-M., Rasera, Y., & Füzfa, A. 2012, MNRAS (in prep)

Davis, M., Efstathiou, G., Frenk, C. S., & White, S. D. M. 1985, ApJ, 292, 371

Erdoğdu, P., Lahav, O., Huchra, J. P., et al. 2006, MNRAS, 373, 45

Lavaux, G., Tully, R. B., Mohayaee, R., & Colombi, S. 2010, ApJ, 709, 483

Rasera, Y., Alimi, J.-M., Courtin, J., et al. 2010, in American Institute of Physics Conference Series, Vol. 1241, American Institute of Physics Conference Series, ed. J.-M. Alimi & A. Füzfa, 1134–1139

Watkins, R., Feldman, H. A., & Hudson, M. J. 2009, MNRAS, 392, 743